

states that the longitudinal coupling,  $J_l$ , changes sign during the transition, but its magnitude is the same on both sides.

Equations (7) and (15) can then be compared directly at the transition temperature:

$$\frac{M_A - M_F}{M_s} = \frac{\tau \ln 2}{8\pi S^2 J_t}. \quad (22)$$

The sublattice magnetization in the antiferromagnetic state is expected to be slightly larger than the magnetization in the ferromagnetic state. The quantity on the right side of (22) would be of the order of  $10^{-2}$  for reasonable choices of the parameters.

*Note added in proof.* A. Yoshimori [Phys. Rev.

130, 1312 (1963)] has derived similar results for antiferromagnetic crystals using a semicontinuum model for the ferromagnetic interaction. A. Narath [Phys. Rev. 131, 1929 (1963)], has extended the measurements on  $\text{CrCl}_3$  to below  $1^\circ\text{K}$  and has found that the approximation  $\omega_{\mathbf{k}} = \omega_0$  introduces errors in the predicted magnetization curve that are larger than the experimental uncertainties.

#### ACKNOWLEDGMENTS

The author wishes to thank Professor C. Kittel for suggesting this problem and for many helpful discussions and comments during the course of its completion. Thanks are also due to Professor T. Nagamiya for valuable suggestions.

### Satellites in the Magnetoplasma Resonance in Sodium\*

J. R. MERRILL, M. T. TAYLOR, AND J. M. GOODMAN†

*Laboratory of Atomic and Solid State Physics, Physics Department, Cornell University, Ithaca, New York*

(Received 14 May 1963)

The low-frequency magnetoplasma resonance ("whistler" or "helicon") has been studied in rectangular parallelepiped samples of Na at  $4^\circ\text{K}$  using improved measuring techniques and higher magnetic fields in order to obtain greater resolution. Structure in the resonance was observed as satellites of the previously reported resonances. The observed frequencies of these satellites fit the simple formula reported earlier.

#### INTRODUCTION

THE magnetoplasma resonance considered in this paper is a dynamic form of the Hall effect, which was first observed in Na at  $4^\circ\text{K}$ .<sup>1</sup> The effect can be observed as a standing, circularly polarized electromagnetic wave in a pure metal sample.<sup>1-4</sup> A detailed study of the frequencies of the resonance in many parallelepiped samples was made by Rose, Taylor, and Bowers.<sup>2</sup> This paper is an extension of that work with higher resolution which has brought to light the existence of satellite structure on the resonances observed previously.

Rose *et al.*<sup>2</sup> considered rectangular parallelepiped samples with sides  $X$ ,  $Y$ , and  $Z$  placed in a large magnetic field along the  $z$  direction. It was assumed that the standing wave pattern in the sample would have an integral number of half-wavelengths in each of the three directions. A series of resonances was observed corre-

sponding to modes with a single half-wavelength in each of the  $x$  and  $y$  directions, but a varying number of half-wavelengths in the  $z$ , or field, direction. Other investigators<sup>3,4</sup> have also reported modes with varying numbers of half-wavelengths along the magnetic field. However, no modes with more than one half-wavelength in either of the directions transverse to the magnetic field have been reported. We shall call such modes "transverse modes." The present work observes and examines the resonant peaks which arise from these transverse modes. These appear as satellites of those peaks observed by previous investigators.

The increased resolution which made this work possible was due to two new features in the instrumentation. First, phase-sensitive detection increased the signal to noise ratio by an order of magnitude<sup>5</sup>; and second, the use of a magnetic field of 27.4 kG produced resonances having a  $Q$  of from 20 to 30 in the very pure Na ( $\rho_{300^\circ\text{K}}/\rho_{4^\circ\text{K}} \approx 7500$ ). This  $Q$  is 3 to 4 times greater than the highest  $Q$ 's previously reported for the magnetoplasma effect.

#### THEORY

The dispersion relation for the magnetoplasma wave propagating in an unbounded metal (neglecting elec-

\* This work was supported by the U. S. Atomic Energy Commission and the Advanced Research Projects Agency.

† National Science Foundation Predoctoral Fellow.

<sup>1</sup> R. Bowers, C. Legendy, and F. E. Rose, Phys. Rev. Letters 7, 339 (1961).

<sup>2</sup> F. E. Rose, M. T. Taylor, and R. Bowers, Phys. Rev. 127, 1122 (1962).

<sup>3</sup> R. G. Chambers and B. K. Jones, Proc. Roy. Soc. (London) A270, 417 (1962).

<sup>4</sup> P. Cotti, A. Quattropani, and P. Wyder, Phys. Cond. Mat. 1, 27 (1963).

<sup>5</sup> M. T. Taylor, J. R. Merrill, and R. Bowers, Phys. Rev. 129, 2525 (1963).

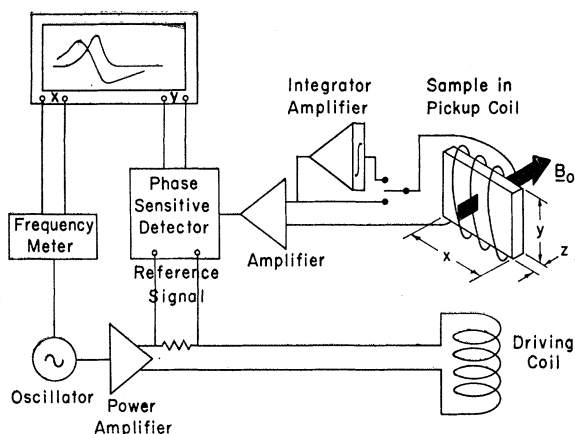


FIG. 1. Schematic diagram of the experiment. The specimen and the two orthogonal coils (pickup coil  $\sim 2000$  turns, driving coil  $\sim 200$  turns) were in liquid He. The magnetic field,  $B_0$ , was 27.4 kG. The phase sensitive detector uses a Hall effect multiplier.

tron scattering<sup>6</sup>) is<sup>1,3</sup>

$$\omega = (RB_0/\mu_0)kk_z \quad (\text{mks units}). \quad (1)$$

$B_0$  is the large magnetic field in the  $z$  direction;  $k_z$ , the  $z$  component of the wave vector  $k$ ;  $R$  is the Hall coefficient; and  $\omega$  is the angular frequency of the magnetoplasma wave.

In order to calculate the resonant frequencies of parallelepiped samples (sides  $X, Y, Z$ ), we use the dispersion relation (1) and fix the wave vector by analogy with standard cavity theory.<sup>2</sup> Hence, the wave vector is assumed to be given by

$$\mathbf{k} = \pi(l/X, m/Y, n/Z),$$

where  $l, m, n$  are integers. It then follows that

$$\omega = \frac{\pi^2 RB_0 n^2}{\mu_0 Z^2} \alpha_{lmn}, \quad (2)$$

where<sup>7</sup>

$$\alpha_{lmn} = \left[ 1 + \left(\frac{l}{n}\right)^2 \left(\frac{Z}{X}\right)^2 + \left(\frac{m}{n}\right)^2 \left(\frac{Z}{Y}\right)^2 \right]^{1/2}.$$

Equation (2) has also been obtained by other workers.<sup>3,4</sup> No rigorous solution for the boundary problem has been reported for finite specimens. The only exact solution of the boundary value problem was given by Chambers and Jones<sup>3</sup> for the special case of a specimen infinite in the  $x$  and  $y$  directions. Equation (2) reduces to their relation in this limit.

#### EXPERIMENTAL APPARATUS

Figure 1 shows a schematic diagram of the apparatus. The specimen in the large magnetic field,  $B_0$ , was surrounded by two orthogonal coils, the pickup and driving

<sup>6</sup> Theories which take electron scattering into account (Refs. 3 and 4) show that the correction for finite resistivity in the present work is 0.02%.

<sup>7</sup>  $\alpha_{lmn}$  corresponds to  $(1/n)G_{lmn}$ , where  $G_{lmn}$  is the geometry factor of Ref. 2.

coils. Both coils were perpendicular to the field  $B_0$  and both were fixed rigidly on the specimen holder.

The large magnetic field,  $B_0 = 27.4$  kG, was produced in a superconducting solenoid. The solenoid has two pounds of Nb-Zr fully insulated wire wound on a 1-in.-diam stainless steel former, which was 6 in. long. The specimen holder was held firmly inside the solenoid by means of phosphor bronze springs. The solenoid was continuously supplied with 18-A direct current from outside the cryostat.

The current from a variable frequency oscillator produced a small magnetic field, of the order of 5G, in the driving coil. The output voltage of the pickup coil exhibited maxima at certain frequencies of the drive field. These were determined by the frequencies for which the magnetoplasma resonance occurred in the sample.

The voltage induced in a 2000 turn pickup coil was approximately 100 mV for the major resonance. For the satellites studied, the voltage ranged down to 100  $\mu$ V. After amplification and phase sensitive detection, the signal delivered to the  $X$ - $Y$  recorder was a few mV.

The phase-sensitive detection with respect to the drive field resolved the resonance into its two components—an absorption curve and a dispersion curve.<sup>5</sup> Only absorption curves were used in this work. Phase-sensitive detection also increased the signal-to-noise ratio by an order of magnitude. The particular phase-sensitive detector used was a Hall effect multiplier.<sup>8</sup>

#### RESULTS

Two qualitatively different types of sample were investigated: Degenerate samples with  $X = Y$ , and non-degenerate samples with  $X \neq Y$ . ( $Z$  was less than both  $X$  and  $Y$  in all samples.) In degenerate samples, Eq. (2) predicts that two distinct modes have the same frequency, namely, the modes  $(l=p, m=q, n)$  and  $(l=q, m=p, n)$ . In nondegenerate samples this degeneracy is removed.

Figure 2 shows a typical result for a degenerate sample. It is a tracing of the original curves obtained on the  $X$ - $Y$  recorder. Note the absence of random noise from the signal; the noise on the original graph paper seldom exceeded the width of the tracing pen line. Only those resonances corresponding to modes with  $n=1$  (that is, with one half-wavelength along the field,  $B_0$ ) are shown. The lowest frequency resonance is the so-called "fundamental." Due to poorer resolution, previous studies did not show any peaks between this fundamental (1,1,1) and the next major peak (1,1,3) which occurs at approximately nine times the fundamental frequency.<sup>9</sup> In the present work, we have re-

<sup>8</sup> We used a model M235T1 Hall effect multiplier with ferrite magnetic circuit available from Instrument Systems Corporation, Halltest Division, College Point, Long Island, New York.

<sup>9</sup> Reference 4, using a different excitation technique, reported observing the major peak (1,1,2) at approximately four times the fundamental frequency.

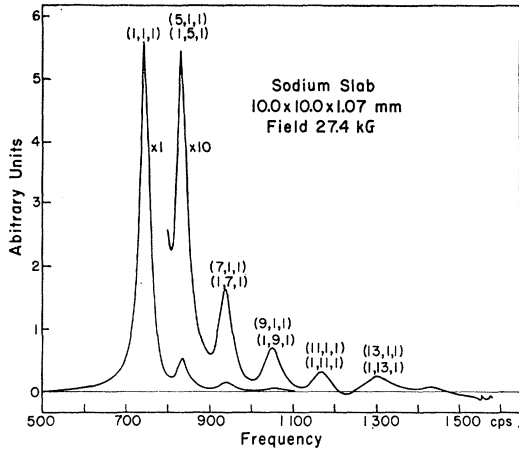


FIG. 2. Typical absorption curve as a function of driving field frequency for a degenerate Na slab. The figure is a tracing of the X-Y recorder chart. The random noise on the original chart is seldom greater than the tracing pen width. The peaks are numbered by their  $(l,m,n)$  designation and the relative gains ( $\times 1$ ,  $\times 10$ ) of the two curves are shown.

stricted our study to the group of modes with  $n=1$  because the fractional frequency separation of the transverse modes is greatest in this group. The groups of resonances with  $n=3$  and  $n=5$  showed satellite structure similar to that of the  $n=1$  group.

The resonant peaks in Fig. 2 are labeled by their  $(l,m,n)$  designations. These designations are determined by considering regularities in both the heights and the frequencies of the observed peaks. An approximate theory of heights<sup>3</sup> predicts that, for our coil geometry, the height of the  $(l,m,n)$  mode should be proportional

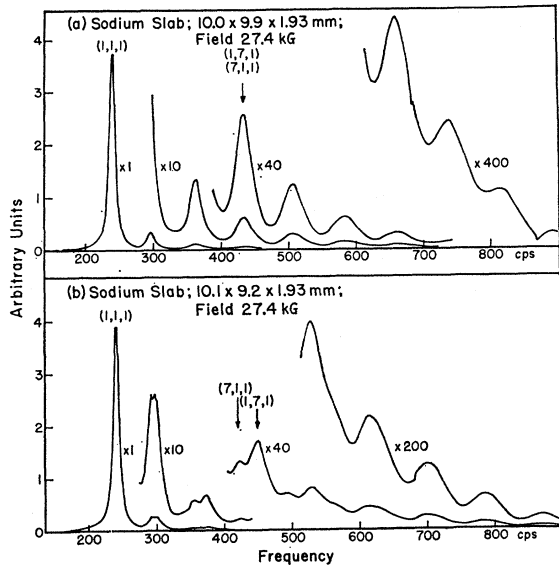


FIG. 3. Comparison of curves for a degenerate sample (a), and a nondegenerate sample (b). The relative gains for the curves are given. The arrows exhibit the splitting of a degenerate peak in (a) into two peaks in (b).

to  $(1/l^2 m^2 n^2)$ , for  $l, m$ , and  $n$  all odd integers, and zero otherwise. This is also to be expected from a simple zone type argument; as the number of half-wavelengths enclosed by the coil increases, the voltage output will decrease because of the flux cancellation. On this basis, the modes can be listed in approximate order of observability. The frequencies of the peaks observed are then compared against the expected frequencies for exact identifications.

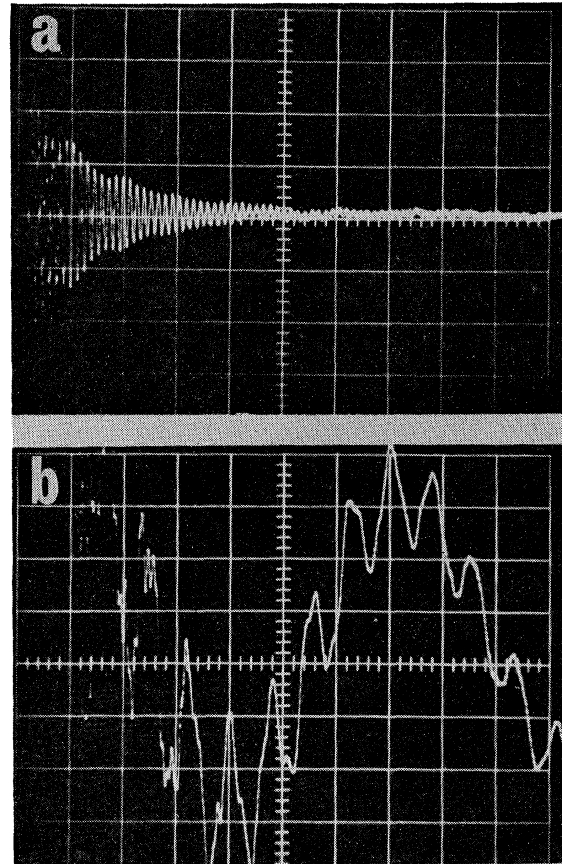


FIG. 4. The voltage in the pickup coil as a function of time on applying a small step field to the sample. The sample is in a large magnetic field of 27.4 kG. The sample dimensions are  $9.0 \times 9.0 \times 1.05$  mm. This is similar to the sample used for Fig. 2. (a) The time scale is 10 msec/div; the vertical scale is 1 mV/div. The beat phenomenon is the interaction of the  $(1,5,1)$  and the  $(1,1,1)$  modes. (b) The first 0.2 div. of (a) with an expanded time scale of 0.2 msec/div. The effects of the  $(1,1,5)$  and  $(1,1,3)$  modes upon the  $(1,1,1)$  fundamental are evident.

The heights of the observed transverse modes in a degenerate sample are monotonic with frequency. In nondegenerate samples, however, this is no longer true. Figure 3(a) shows another degenerate sample; Fig. 3(b) shows a nondegenerate sample of almost the same size. The arrows indicate the splitting of a degenerate peak. This splitting is apparent for most of the peaks observed.

Nondegenerate samples down to  $10 \text{ mm} \times 5 \text{ mm} \times 1$

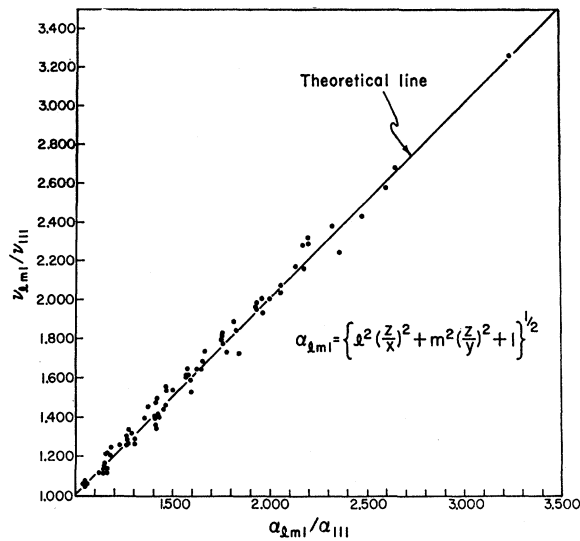


FIG. 5. Comparison between observed frequency ratios,  $\nu_{lm1}/\nu_{111}$ , and those calculated from sample geometry,  $\alpha_{lm1}/\alpha_{111}$ . 83 resonances from 13 samples were measured.

mm and  $10 \text{ mm} \times 5 \text{ mm} \times 2 \text{ mm}$  were run during the experiments.

In our high  $Q$  samples, the effect of transverse modes can be seen by the earliest detection technique—the so-called “decay method.”<sup>1,4</sup> In this technique one observes the voltage induced in the pickup coil as a function of time after a small step field is produced in the drive coil. The result is an oscillatory decay due to the sample resonances. Figures 4(a) and (b) show such decaying oscillations for a sample similar to that of Fig. 2. The envelope of the oscillation in Fig. 4(a) is not a simple exponential, but shows fluctuations due to the (1,5,1) mode beating with the (1,1,1) fundamental.

Figure 4(b) is the first portion of Fig. 4(a) with an expanded time scale. Apparent in this figure is the presence of the (1,1,3) and (1,1,5) modes in addition

to the fundamental mode (1,1,1). These modes are members of the series studied by previous investigators using the resonance technique.

#### DISCUSSION

The results of this work can be analyzed by comparing the observed frequencies with those calculated from the sample dimensions. In Fig. 5 this is done for 13 different samples and 83 separate resonances. In order to remove from consideration the effects of uncertainties in the field,  $B_0$ , and the Hall coefficient,  $R$ , ratios of frequencies were taken. For each experimental run, we calculated the ratio of the frequency of the transverse mode ( $l, m, 1$ ) to that of the fundamental. For comparison with theory we used the relation obtained from Eq. (2)

$$\nu_{lm1}/\nu_{111} = \alpha_{lm1}/\alpha_{111},$$

where  $\nu_{lmn}$  is the observed frequency and  $\alpha_{lmn}$  is calculated from the sample dimensions and the assigned  $l$  and  $m$  values. The scatter of the points is no larger than expected from inaccuracies in the determination of Na sample dimensions.

Our interpretation of the results has been based upon the dispersion relation (2) combined with a physically reasonable criterion of the relative observability of modes. The agreement of the experimental points with the theoretical line in Fig. 5 verifies our interpretation.

The results of this work complement those of Ref. 2, and the two papers together demonstrate that Eq. (2) represents accurately the observed positions of both major and satellite peaks in the resonance spectrum. It remains for this mode formula to be placed on a firmer theoretical basis.

#### ACKNOWLEDGMENTS

The authors would like to thank R. Bowers for helpful discussions and S. Tallman for contributions to the experiment.

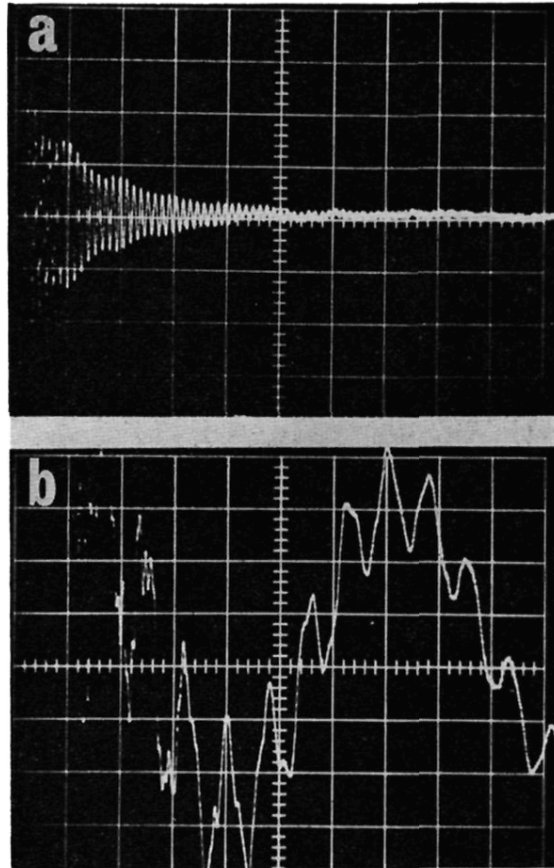


FIG. 4. The voltage in the pickup coil as a function of time on applying a small step field to the sample. The sample is in a large magnetic field of 27.4 kG. The sample dimensions are  $9.0 \times 9.0 \times 1.05$  mm. This is similar to the sample used for Fig. 2. (a) The time scale is 10 msec/div; the vertical scale is 1 mV/div. The beat phenomenon is the interaction of the (1,5,1) and the (1,1,1) modes. (b) The first 0.2 div. of (a) with an expanded time scale of 0.2 msec/div. The effects of the (1,1,5) and (1,1,3) modes upon the (1,1,1) fundamental are evident.